Insights into the Stability of Native and Partially Folded States of Ubiquitin: Effects of Cosolvents and Denaturants on the Thermodynamics of Protein Folding†

Muriel Jourdan and Mark S. Searle*

School of Chemistry, University of Nottingham, University Park, Nottingham NG7 2RD, U.K.

Received April 16, 2001; Revised Manuscript Received June 9, 2001

ABSTRACT: The thermodynamics of the native↔A state and native↔unfolded transitions for ubiquitin have been characterized in detail using the denaturants methanol and guanidinium chloride (Gdn·HCl) both separately and in combination. Gdn·HCl destabilizes the partially folded alcohol-induced A state such that the effects of alcoholic solvents on the native↔unfolded transition can be investigated directly via a two-state model. The combined denaturing effects of methanol and Gdn·HCl appear to conform to a simple additive model. We show that ubiquitin folds and unfolds cooperatively in all cases, forming the same "native" state; however, the thermodynamics of the N↔U transition change dramatically between alcoholic and Gdn·HCl solutions, with folding in aqueous methanol associated with large negative enthalpy and entropy terms at 298 K with a gradual falloff in ΔC_p at higher methanol concentrations, as previously reported for the N↔A transition (Woolfson, D. N., Cooper, A., Harding, M. M., Williams, D. H., and Evans, P. A. (1993) *J. Mol. Biol. 229*, 502−511.). Both the N↔U and the N↔A transitions are enthalpy driven to a similar extent. We conclude that under these conditions van der Waals interactions in the packing of the nonpolar protein core, which is common to both the N↔U and the N↔A transitions, appear to drive folding in the absence of entropic effects associated with release of ordered solvent (hydrophobic effect). Solvent transfer studies of hydrocarbons into alcoholic solvents, with and without Gdn·HCl, are consistent with a large enthalpic driving force for burial of a nonpolar surface, with a linear dependence of protein stability ($\Delta G_{N\leftrightarrow U}$) on cosolvent concentration reflected in a similar linear dependence of hydrocarbon solubility. The data demonstrate that the hydrophobic effect is not a prerequisite for specific stabilization of the native state or the A state and that van der Waals packing of the nonpolar core appears to be the dominant factor in stabilization of the native state.

Under native folding conditions, protein stability represents a small energetic difference between a large number of opposing factors that marginally favor the folded state over the unfolded state. The nature and magnitude of the individual contributing interactions are highly dependent on the solvent environment and its effects on the stability of the unfolded polypeptide chain. Consequently, chemical denaturants and cosolvents can readily tip the balance in favor of the unfolded state, providing valuable tools for probing protein stability (*1*, *2*). Guanidinium chloride (Gdn·HCl)[1] is thought to bind to the polypeptide chain through hydrogen bonding so as to stabilize preferentially the unfolded state, where more amide groups are exposed. High concentrations of denaturant are required to compete effectively with binding sites occupied by water (*3*, *4*). Furthermore, urea appears to increase the solubility of hydrocarbons in water, suggesting that an alternative mechanism may be a partial reduction in the hydrophobic contribution to folding. Calorimetric studies of the dissolution of cyclic dipeptides in denaturants concluded that both mechanisms contribute (*5*).

While alcohols (notably, TFE and methanol) have been widely used to enhance the intrinsic secondary structure propensity (α-helix and β-sheet) of peptides that fold only weakly in water (*6*−*15*), they have a denaturing effect on protein structure. This property appears to arise from an ability to disrupt tertiary interactions while inducing a nonnative α-helical structure (*16*−*20*). The predominance of local secondary structure interactions rather than tertiary contacts in these alcohol-induced partially folded states suggests that they may advance some insight into the interactions present early on in the folding process.

More recently, the effects of cosolvents on the kinetics of protein folding↔unfolding have been used to probe the structure of folding transition states, partly because TFE promotes α-helical and β-sheet secondary structure formation

† This work was funded by a European Commission Marie Curie Research Fellowship to M.J. The EPSRC of the U.K. and School of Chemistry, Nottingham, funded the NMR and CD facilities.

* Corresponding author tel: 0115 951 3567; fax: 0115 951 3564; e-mail: mark.searle@nottingham.ac.uk.

[1] Abbreviations: Gdn·HCl, guanidinium chloride; TFE, trifluoroethanol; $\Delta G_{N\leftrightarrow U}$, free energy change for the transition from the native state (N) to the unfolded state (U); $\Delta H_{N\leftrightarrow U}$, enthalpy change for the transition from the N state to the U state; $\Delta S_{N\leftrightarrow U}$, entropy change for the transition from the N state to the U state; $\Delta G_{N\leftrightarrow A}$, free energy change for the transition from the N state to the partially unfolded A state; $\Delta H_{N\leftrightarrow A}$, enthalpy change for the transition from the N state to the partially unfolded A state; $\Delta S_{N\leftrightarrow A}$, entropy change for the transition from the N state to the partially unfolded A state; ΔC_p, change in heat capacity.

10.1021/bi010767j CCC: $20.00
Published on Web 08/02/2001

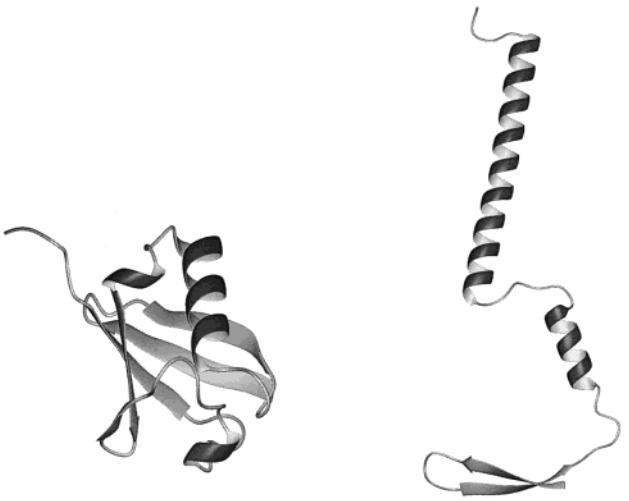

FIGURE 1: (left) Structure of the N state of ubiquitin from the X-ray coordinates (1ubq; *33*); (right) model of the A state of ubiquitin in 60% methanol at low pH (adapted from *37*). Structures drawn with the program MOLMOL (*57*).

but also because it weakens tertiary and quaternary interactions (*21*−*25*). The effects on the kinetics of protein folding using TFE are not clear-cut; notable effects are observed in some cases in speeding up folding rates but not in others, casting doubts on the generality of any conclusions regarding the usefulness of cosolvents in probing folding kinetics because of distortions to the transition state and its position along the folding pathway (*23*−*25*). Others have proposed a correlation between the effects of TFE on folding kinetics and the number of local backbone hydrogen bonds formed in the transition state (*24*).

There is general interest in determining the mechanism by which these various cosolvents and denaturants modulate secondary structure stability, on one hand, and disruption of protein tertiary interactions, on the other (*26*−*28*). The relationship between stability and specificity for a particular folded state and the nature and distribution of the stereochemical code that defines a particular conformation and its ability to cooperatively self-assemble (*29*) remain fundamental questions. A detailed description of the effects of cosolvents on the thermodynamics of folding is a step toward elucidating their mechanism of action and dissecting the various energetic contributions that account for the protein stability and the specificity of the folded state (*30*−*32*).

We have investigated the stability and thermodynamics of folding of bovine ubiquitin under a variety of nonphysiological conditions. Ubiquitin is a 76 residue protein, free of disulfide bonds and bound cofactors, for which high-resolution structures have been determined by both X-ray and NMR (*33*−*35*). Alcoholic cosolvents (both TFE and methanol) have been shown to induce a partially unfolded state at low pH (A state) in which a high proportion of secondary structure (both native and non-native) is stabilized in the absence of significant tertiary interactions (*20*, *36*, *37*). The A state is represented by three loosely coupled segments of secondary structure with enhanced internal mobility (see Figure 1) (*37*). Calorimetric analysis has shown that the N↔A state transition can occur in methanol (>30% v/v) in the absence of any significant change in heat capacity, suggesting that folding to the native state (N↔A) is not critically dependent on the solvent-ordering effects normally associated with the hydrophobic effect (*38*).

In the current study, we have characterized in detail the thermodynamics of the N↔A and N↔U transitions using methanol and Gdn·HCl separately, and in combination, to probe the energetics of folding at a T_m of 298 K. We show that Gdn·HCl destabilizes the partially folded A state such that the effects of alcoholic solvents on the N↔U transition can be investigated directly via a two-state model. We show that ubiquitin folds and unfolds cooperatively in all cases, forming the same "native" state; however, the thermodynamics of the N↔U transition changes dramatically between alcoholic and Gdn·HCl solutions. The thermodynamic profile shows that folding in aqueous methanol is associated with a large negative enthalpy and entropy of folding at 298 K and negligible change in heat capacity ($\Delta C_p \approx 0$) that appears to reflect the contribution from van der Waals interactions in the packing of the protein core in the apparent absence of the entropic advantage from the hydrophobic effect as previously noted for the N↔A transition under similar conditions (*38*). The enthalpically driven formation of core nonpolar interactions promotes folding, demonstrating that the hydrophobic effect is not a prerequisite for specific stabilization of the native state.

MATERIALS AND METHODS

Materials. Bovine ubiquitin, ultrapure Gdn·HCl, CD_3OD, and spectroscopic grade CH_3OH were purchased from Sigma and used without further purification. Gdn·HCl concentrations were determined by refractive index measurements (*2*).

NMR Methods. All 1D ^{1}H NMR experiments were performed on a Bruker DRX500 spectrometer. Solvent suppression was achieved by presaturation. Data were processed on a Silicon Graphics Indy Workstation using Bruker XWINNMR software. For ubiquitin folding/unfolding studies, protein concentrations in methanol solutions were typically 0.25 mM, while those in Gdn·HCl/methanol mixtures were between 0.2 and 0.4 mM. Low concentrations of protein were used to avoid aggregation problems in the unfolded state.

Circular Dichroism Spectroscopy. Circular dichroism (CD) spectra were acquired using an Applied Photophysics pi-star 180 system, using a 0.2 cm path length cell. Stock solutions of protein were prepared as 1 mg in 1 mL of solution. Samples were diluted with water or aqueous methanol to give 6 μM solutions for analysis by CD. Typically, 10 scans were acquired over the wavelength range of 190−250 nm in 1.0 nm steps using a bandwidth of 4 nm at 298 K. The resulting data were averaged, smoothed, and baseline corrected by solvent subtraction.

Thermodynamic Analysis. A two-state model for the ubiquitin folding transition was assumed with $\Delta G_{N\leftrightarrow U}$ calculated from $-RT \ln K_{eq}$, where the equilibrium constant, K_{eq}, equals $f_F/(1 - f_F)$ and f_F is the fraction folded. The temperature dependence of $\Delta G_{N\leftrightarrow U}$ enabled $\Delta H_{N\leftrightarrow U}$, $\Delta S_{N\leftrightarrow U}$, and ΔC_p to be determined at 298 K by fitting the following expression using a nonlinear least-squares analysis (Kaleidagraph software v3.0, Synergy, Inc.):

$$\Delta G_{N\leftrightarrow U} = [\Delta H_{N\leftrightarrow U} + \Delta C_p(T - 298)] - T[\Delta S_{N\leftrightarrow U} + \Delta C_p \ln(T/298)] \quad (1)$$

Table 1: Thermodynamics of Folding (N↔U) for Ubiquitin at 298 K (pH 4) in Guanidinium Hydrochloride/Methanol Mixtures

[MeOH][a] (M)	denaturant [Gdn·HCl] (M)	$\Delta H_{N\leftrightarrow U}$ (kJ mol^{-1})	$\Delta S_{N\leftrightarrow U}$ (J K^{-1} mol^{-1})	ΔC_p (J K^{-1} mol^{-1})
0	3.90	+9.8 (±1.5)	31.3 (±5)	−5180 (±244)
2.46 (10%)	3.51	−21.0 (±3.1)	−70.4 (±10)	−8407 (±496)
4.92 (20%)	3.15	−77.1 (±3.6)	−257 (±12)	−6597 (±504)
7.34 (30%)	2.82	−92.3 (±4.6)	−312 (±16)	−4368 (±650)
9.78 (40%)	2.22	−145.3 (±9.4) (**−137.7**)	−487 (±31) (**−462**)	−2567 (±2051)
12.30 (50%)	1.75	−180.0 (±7.6) (**−168.3**)	−604 (±26) (**−565**)	−2489 (±2678)

[a] Concentrations are also given as percentage values (v/v). Numbers in bold (40 and 50% methanol) represent enthalpies and entropies determined assuming a linear correlation ($\Delta C_p = 0$) between $\Delta G_{N\leftrightarrow U}$ and T ($R > 0.99$ in all cases) by NMR. Only the data for folding in 0, 10, 20, and 30% methanol show significant curvature (nonzero ΔC_p; see Figure 3) and were fitted using eq 1. Uncertainties in thermodynamic parameters are derived from fitting errors.

Table 2: Thermodynamics of the N↔A Transition for Ubiquitin at 298 K in Methanol

[MeOH][a] (M)	pH	$\Delta H_{N\leftrightarrow A}$ (kJ mol^{-1})	$\Delta S_{N\leftrightarrow A}$ (J K^{-1} mol^{-1})
4.92 (20%)	1.9	−37 (±20)	−103 (±7)
7.34 (30%)	1.9	−246.9 (±54) (**−315**)	−803 (±182) (**−1031**)
9.78 (40%)	2.0	−216 (±8) (**−226**)	−720 (±27) (**−755**)
12.30 (50%)	3.1	−242 (±6) (**−247.6**)	−809 (±26) (**−826**)

[a] Concentrations are also given as percentage values (v/v). Numbers in bold represent enthalpies and entropies determined by NMR, assuming a linear correlation ($\Delta C_p = 0$) between $\Delta G_{N\leftrightarrow A}$ and T ($R > 0.99$ in all cases). Only the data for folding in 20% methanol show significant curvature (see Figure 6), and this was fitted using eq 1.

Values for $\Delta G_{N\leftrightarrow U}$ were determined directly from the integration of peak intensities in the NMR spectrum and are subject to relatively small uncertainties (≈5%). A similar approach was used to determine the thermodynamics of the N↔A transition. The resonances for Hϵ of His68 and Hδ and Hϵ of Tyr59 are clearly resolved for both the unfolded and the folded states and were used to estimate populations. Similar populations were obtained in each case with no obvious distortions due to differential relaxation rates caused by differences in local dynamic behavior in the folded vs unfolded state. Errors in the thermodynamic parameters in Table 1 are fitting errors. Parameters were determined from a number of arbitrary starting values, and all converged to the same final values ($R > 0.98$). Values for ΔC_p calculated for ubiquitin folding in high concentrations of methanol (>30% v/v) are subject to much larger errors as a consequence of intrinsically large values for $\Delta H_{N\leftrightarrow U}$. Fitting the data in 40 and 50% methanol to a simple linear temperature dependence gave only a marginally worse fit than allowing a nonzero value for ΔC_p (Table 1). One point or a small number of points could have a large impact on the iteratively determined value for ΔC_p but only a small impact on the enthalpy and entropy parameters (see Tables 1 and 2).

Solubility Studies of Toluene in Mixed Solvents. The solubility of toluene in aqueous solutions containing various concentrations of methanol and Gdn·HCl was determined spectrophotometrically by UV absorption ($\epsilon_{268} = 225$ M^{-1} cm^{-1} or $\epsilon_{261} = 173$ M^{-1} cm^{-1} following the method previously described by Woolfson et al.) (*38*). A Cecil 8000 series UV spectrophotometer was used with a thermostated cell housing temperature regulated by a Grant water circulator bath. Sample temperatures were measured from a reference cell containing the same solvent mixture. The concentration of toluene in the aqueous phase was measured under conditions in which two distinct layers could be observed in the cell. Experiments used a 0.1 cm cell in which 80 μL of toluene was layered on top of 200 μL of solvent at pH 2.0. The sample was first allowed to equilibrate to the required temperature (≈30 min), and the mixture was agitated several times and reequilibrated for 10 min before the UV absorbance was measured. ΔG_{trans} (free energy of transfer from toluene into aqueous solution) was calculated according to $\Delta G_{trans} = -RT \ln X_T$, where X_T is the mole fraction of toluene in solution. The curvature in the plot of ΔG_{trans} vs T was then fitted using an analogous expression to eq 1.

RESULTS

Stability of Ubiquitin in Gdn·HCl. Ubiquitin is a highly stable protein at neutral pH, undergoing thermal denaturation above 100 °C. Denaturants such as urea and Gdn·HCl depress the T_m significantly such that at pH 4 ubiquitin cooperatively and reversibly unfolds with a T_m of ≈ 298 K in the presence of ≈4 M Gdn·HCl. The protein unfolding process can be monitored by ^{1}H NMR, since the N (native) and U (unfolded) states are in slow exchange over a wide range of temperatures (*39*, *40*). The Hϵ of His 68 (8.86 ppm for the N state) splits into two signals, the relative intensities of which can be used directly to estimate $\Delta G_{N\leftrightarrow U}$. We have shown previously that the temperature dependence of the populations of the N and U states (and hence $\Delta G_{N\leftrightarrow U}$) can be used to estimate the enthalpy and entropy of folding (*40*). Under these conditions (pH 4, 4 M Gdn·HCl), ubiquitin undergoes cold denaturation below 298 K; the highly curved plot of $\Delta G_{N\leftrightarrow U}$ vs T is indicative of a large change in heat capacity (ΔC_p) on folding and a positive entropy and enthalpy term. Fitting the data to eq 1 (see NMR Methods), which allows for the temperature dependence of the enthalpy and entropy terms, shows that folding is entropy driven at 298 K under these conditions (Table 1). For fitting purposes, ΔC_p was assumed to be independent of temperature over the relatively narrow range studied. Recent calorimetry studies have also shown that ubiquitin undergoes cold denaturation under similar conditions (*41*) and that the enthalpy and entropy terms change sign (becoming positive) around 293 K, in good agreement with our analysis.

The linear extrapolation method was used to estimate the pH-dependent stability of ubiquitin in water alone from the denaturant-induced sigmoidal unfolding curves, which we interpret in terms of a two-state model. The midpoint of the unfolding transition occurs around 3.5−4 M Gdn·HCl and is largely independent of pH with $\Delta G_{water} = -31(\pm 1)$ kJ mol^{-1} at 298 K over the pH range of 2.9−5.0. In contrast, calorimetry results from a number of studies of ubiquitin (*42*) and the complexation of ubiquitin peptide fragments

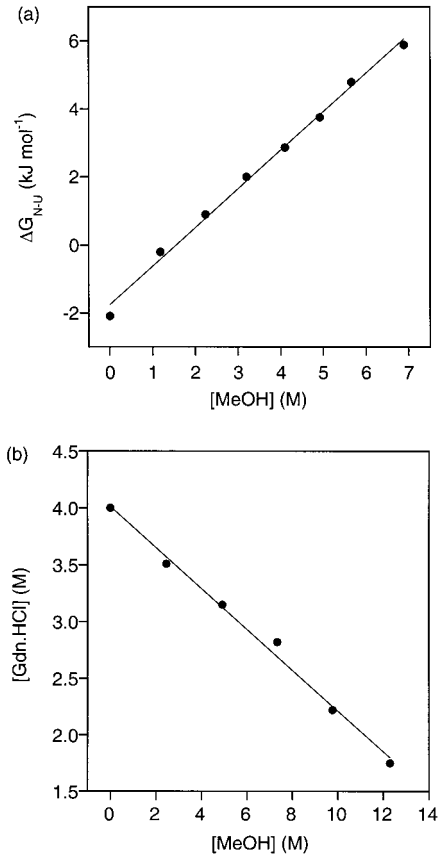

FIGURE 2: (a) Effects of methanol concentration on the stability of ubiquitin in 3.6 M Gdn·HCl at pH 4.0, estimated from the population of the folded and unfolded states by NMR; (b) relationship between the denaturing effects of Gdn·HCl and methanol with each data point corresponding to $\Delta G_{N\leftrightarrow U} = 0$.

(*40*), in which thermal denaturation was performed in the absence of denaturants, show a marked pH dependence. The data suggest that denaturants are highly effective in screening surface electrostatic interactions that otherwise contribute to protein stability through salt bridges. The ability of the guanidinium group to bind to surface-exposed carboxylate groups would appear to negate any pH-dependent effects on protein stability associated with changes in ionization states of specific residues.

Effects of Methanol on the N↔U Transition. We have used the NMR approach to determine the thermodynamics of folding under a variety of conditions. The effect of methanol on the stability of ubiquitin has been investigated by making small additions of the cosolvent to a 3.6 M Gdn·HCl solution of the protein at 298 K. The change in the population of the folded and unfolded states was monitored from the NMR signals of His 68; the correlation between $\Delta G_{N\leftrightarrow U}$ vs [CH_3-OH] is illustrated in Figure 2a. The added cosolvent destabilized ubiquitin by ≈8 kJ mol^{-1} over the range of 0−30% v/v (0−7 M). In separate experiments, we estimated the enthalpy and entropy of folding of ubiquitin at a number of different methanol concentrations over a similar range (0−50% v/v). In each case, Gdn·HCl was added stepwise to the protein at pH 4 and 298 K in the presence of a fixed concentration of methanol until the midpoint of the folding transition was reached, where only two species were evident in solution ($\Delta G_{N\leftrightarrow U} = 0$ at 298 K; N and U states equally populated). The folded state showed exactly the same NMR

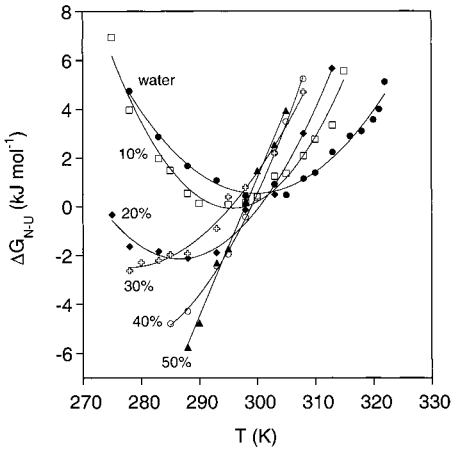

FIGURE 3: Temperature−stability plots for ubiquitin in various concentrations of methanol in the range of 0−12 M (0−50% v/v), derived from NMR estimates of the population of the folded state. Lines of best fit to eq 1 are shown, except for the data for 50% methanol for which a linear correlation was assumed.

characteristics over a wide range of solvent conditions indicating that the protein is folding to the same native state, excluding the possibility of multiple isoenergetic states with different secondary and tertiary folds. The relationship between [Gdn·HCl] and [MeOH], corresponding to $\Delta G_{N\leftrightarrow U} \approx 0$, is shown in Figure 2b. The temperature dependence of the folded population was then estimated for samples containing 10, 20, 30, 40, and 50% (v/v) methanol (in addition to that for water alone), and the data were fitted as described to estimate $\Delta H_{N\leftrightarrow U}$, $\Delta S_{N\leftrightarrow U}$, and ΔC_p for folding at 298 K (Table 1). A number of temperature−stability plots are shown in Figure 3. Cold denaturation of ubiquitin is evident in methanol up to 30% (v/v), with folding becoming increasingly enthalpy driven. The curvature of the temperature−stability plot also decreases, indicating a reduction in ΔC_p for the folding transition with the plot of $\Delta G_{N\leftrightarrow U}$ vs T becoming essentially linear for 50% v/v methanol (see Figure 3).

While the data in Figure 2 show that the change in the free energy of folding ($\Delta G_{N\leftrightarrow U}$) after addition of methanol is modest, the change in stability underlies a very large change in compensating enthalpy and entropy terms for folding. $\Delta H_{N\leftrightarrow U}$ in water alone has been shown to be endothermic (+9.8 kJ mol^{-1}); however, in 50% methanol, folding is strongly enthalpy driven with $\Delta H_{N\leftrightarrow U} = -180$ kJ mol^{-1}, increasing linearly over this concentration range (Figure 4). The change in entropy on folding compensates strongly to ensure that $\Delta G_{N\leftrightarrow U}$ remains a small difference between two large opposing terms. By adjusting the T_m for the unfolding transition to lie close to 298 K, we are able to determine the thermodynamics of folding at this temperature without introducing large extrapolation errors.

NMR analysis of chemical shifts and CD studies of the unfolding transition confirmed that we are observing the N↔U process in the presence of Gdn·HCl and methanol rather than the N↔A transition previously described in methanol alone (*38*). This is particularly evident from the CD data where the A state is characterized by a strong α-helical signal, corresponding to induced non-native structure in the C-terminal half of the partially folded state (Figure 5a). At pH 2, the native state of ubiquitin is stable up to 40% methanol, above which a transition is observed to the

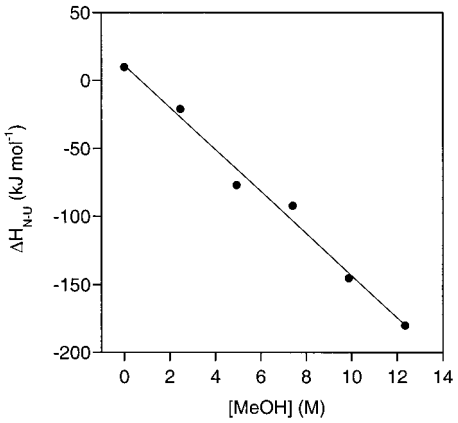

FIGURE 4: Enthalpy of folding for the N↔U transition vs methanol concentration derived from NMR analysis of the temperature−stability profiles shown in Figure 3.

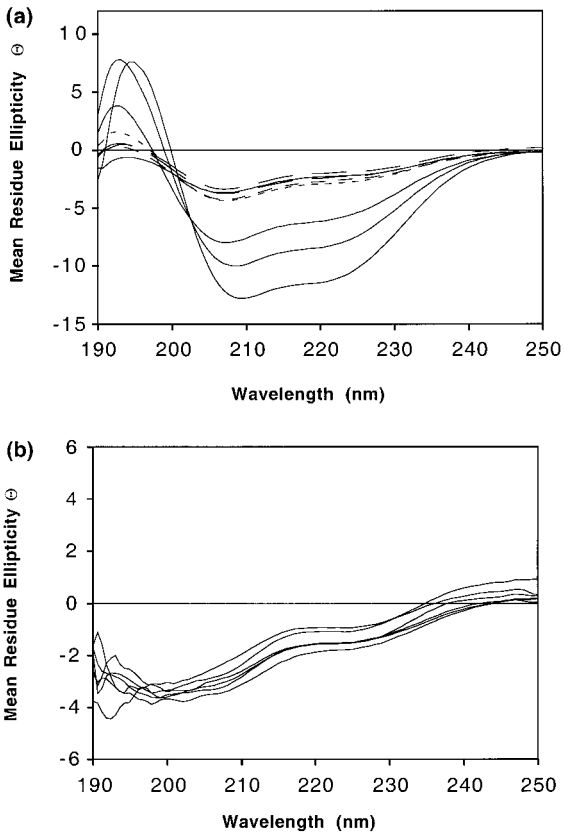

FIGURE 5: (a) CD spectra of ubiquitin collected at 290 K and pH 2.0 at various concentrations of methanol (0, 10, 20, 30, 40, 50, 60, and 100% in order of increasing ellipticity at 222 nm) illustrating the N↔A transition above 50% v/v cosolvent as evident from the large increase in ellipticity at 208 and 222 nm; (b) CD spectra of ubiquitin in various compensating ratios of Gdn·HCl and methanol for which $\Delta G_{N\leftrightarrow U} = 0$ (N and U states equally populated). Spectra correspond to each of the data points shown in Figure 2a up to a [MeOH] of 12.35 M (50% v/v). All protein concentrations are 6 μM; mean residue ellipticity in deg cm^2 dm^{-1} × 10^{-3}.

partially folded state. Significantly, the α-helical content of the polypeptide chain continues to increase up to ≈100% methanol, suggesting that the A state is not a discrete thermodynamic entity but that its secondary structure content continues to be enhanced by the effects of cosolvent. In Figure 5b, the CD spectra illustrate the combined denaturing effects of both methanol and Gdn·HCl on ubiquitin. The experimental conditions were chosen using different ratios of the two denaturants to ensure that the N and U states in all cases are equally populated, analogous to the data shown in Figure 2b determined by NMR. The CD spectra are very similar over the range of 0−50% methanol; the absence of a strong absorbance at 222 nm demonstrates that in the presence of Gdn·HCl as the co-denaturant the A state is destabilized even in the presence of high concentrations of methanol and that only the N and U states are present in equilibrium.

Additive Effects of Gdn·HCl and Methanol on Ubiquitin Stability. We have shown that Gdn·HCl and methanol destabilize the folded state. While methanol alone at low pH has been shown to cause the N state to partially unfold in favor of the A state, there is no evidence for A state formation in the presence of Gdn·HCl, enabling us to characterize the effects of cosolvent on the N↔U reaction. The question remains whether these two denaturants work in an independent additive sense or whether the effects of one are modulated by the other. Starting with the assumption of a simple additive model, then by analogy with the linear extrapolation approach

$$\Delta G_{N\leftrightarrow U} = \Delta G_{water} - m'[\text{Gdn·HCl}] - m''[\text{MeOH}] \quad (2)$$

where m' and m'' are the linear dependences of the free energy change on [Gdn·HCl] and [MeOH], respectively. If [Gdn·HCl] and [MeOH] are balanced over a range of compensating concentrations for which $\Delta G_{N\leftrightarrow U} = 0$ at 298 K, then eq 1 simplifies to

$$m'[\text{Gdn·HCl}] = -m''[\text{MeOH}] + \Delta G_{water} \quad (3)$$

with further rearrangement leading to

$$[\text{Gdn·HCl}] = -(m''/m')[\text{MeOH}] + \Delta G_{water}/m' \quad (4)$$

The simple additive model, represented by eq 4, predicts that the concentration of the denaturants should be linearly correlated with a slope of m''/m' and an intercept of $\Delta G_{water}/m'$. This is observed experimentally, as shown in Figure 2b, under conditions where $\Delta G_{N\leftrightarrow U} \approx 0$. From these data, we estimate that $m' = -7727$ J mol^{-1} M^{-1} and $m'' = -1390$ J mol^{-1} M^{-1}, taking ΔG_{water} at pH 4.0 $= -31$ kJ mol^{-1}, as previously described (*40*).

Using the linear extrapolation method for ubiquitin denaturation in the presence of Gdn·HCl alone, we can estimate m' directly from eq 5:

$$\Delta G_{N\leftrightarrow U} = \Delta G_{water} - m'[\text{Gdn·HCl}] \quad (5)$$

This gives $m' = -7960$ J mol^{-1} M^{-1}, in agreement with the results of others (*41*, *43*). Thus, independent estimates of m' (the concentration-dependent effect of Gdn·HCl on protein stability) in the presence and absence of MeOH give similar values. Conversely, from the data in Figure 2, where $\Delta G_{N\leftrightarrow U}$ is plotted against [MeOH] at a fixed concentration of Gdn·HCl (3.6 M), we estimate a value for m'' of -1137 J mol^{-1} M^{-1}, in good agreement with the value above. The data suggest that the effects of the two denaturants can be approximated by a simple additive model and that the cosolvent does not significantly perturb the effects of Gdn·HCl as a denaturant. The relative m values, however, show that Gdn·HCl is significantly more potent as a denaturant

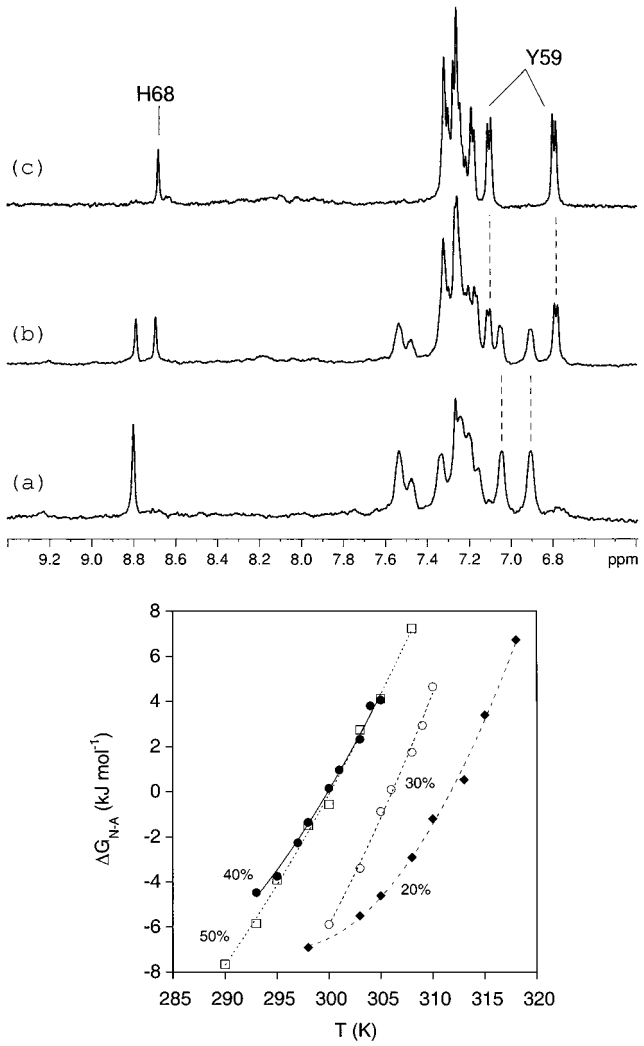

FIGURE 6: (top) ^{1}H NMR spectra (500 MHz) of the N↔A transition in 40% methanol at pH 2.0; (a) N state at 288 K; (b) N and A state equally populated at 300 K; and (c) A state fully populated at 318 K. (bottom) Temperature−stability profiles ($\Delta G_{N\leftrightarrow A}$ vs T) for the N↔A transition at various concentrations of methanol (20, 30, 40, and 50% v/v). Lines of best-fit to eq 1 are shown.

than methanol. In other cases, *m* values for Gdn·HCl and TFE correspond quite closely, though perhaps coincidentally. This is not the case for hen lysozyme, where *m* values are also found to be different for different alcohols (*22*). The potencies of different alcohols as denaturants are also reflected in their different potencies in inducing secondary structure with the hydrocarbon component playing a key role (*27*). The slope of the solvent-induced stability curve for the helical peptide U(21−35) from ubiquitin in the presence of TFE and MeOH shows that the two solvents have different helix-inducing potencies with TFE much more effective (data not shown).

Thermodynamics of the N↔A Transition. At low pH, addition of methanol results in the partial unfolding of ubiquitin to the A state, which is readily monitored by NMR through the appearance of a new set of resonances slightly displaced from those of the N state (Figure 6a). This is most clearly evident for Hϵ of His 68 at 8.8 ppm. The coexistence of two sets of signals shows the two conformations to be in slow exchange, which enabled the thermodynamics of the N↔A state transition ($\Delta H_{N\leftrightarrow A}$, $\Delta S_{N\leftrightarrow A}$, and ΔC_p) to be determined from the temperature dependence of the relative populations using eq 1 (see Table 2). For the N↔A transition, it was more difficult to adjust both pH and methanol concentration to bring the midpoint of the folding transition down to ≈298 K, particularly at low concentrations of cosolvent. The A state could not be populated below 20% methanol. The data in Figure 6b show that the N↔A transition has a marked temperature dependence in aqueous methanol. While $\Delta G_{N\leftrightarrow A}$ vs T shows significant curvature in 20% methanol, the plots become essentially linear in 30−50% methanol, indicating that ΔC_p is significantly diminished under these conditions, in agreement with the conclusions of Woolfson et al. (*38*). Fits to the latter data, assuming a simple linear temperature dependence of $\Delta G_{N\leftrightarrow A}$ ($\Delta C_p = 0$), gave very similar estimates for the enthalpies and entropies for the N↔A transition (see Table 2). Determination of $\Delta H_{N\leftrightarrow A}$ shows that the transition is associated with a large enthalpy change in forming the native state with $\Delta H_{N\leftrightarrow A} = -216$ kJ mol^{-1} with a T_m of 300 K at pH 2.0 in 40% methanol. This is consistent with earlier calorimetry data that also indicate that $\Delta C_p \approx 0$ in 40% methanol, with an estimated enthalpy of folding of −198(±30) kJ mol^{-1} (*38*), showing the close agreement between calorimetric and van't Hoff enthalpies (*44*). Notably, $\Delta H_{N\leftrightarrow A}$ appears to vary little between 30 and 50% methanol, while in contrast $\Delta H_{N\leftrightarrow U}$ appears to vary linearly with methanol concentration.

Insights from Hydrocarbon Solubility Studies. Studies of the solubility of model compounds have been used widely to dissect the thermodynamic contributions to protein folding and unfolding (*5*, *45*−*47*). The effects of methanol on the solvent-ordering contribution to the hydrophobic effect have been examined by Woolfson et al. (*38*) from temperature-dependent studies of the solubilty of toluene. A distinctly curved plot of the free energy of transfer to water, indicating a positive ΔC_p, together with a large unfavorable entropy term are consistent with the solvent-ordering effects associated with the hydrophobic interaction. In contrast, in 40% methanol/60% water, the plot is essentially linear, demonstrating a significant diminution of this effect. The data also show that the free energy of transfer is less unfavorable than in water (≈5 kJ mol^{-1} at 298 K) but that the transfer is now enthalpically unfavorable with a much smaller entropic term, further demonstrating the reduction in the unfavorable solvent-ordering effects. It is particularly notable that the transfer of toluene to 40% methanol is largely an enthalpically unfavorable process. Nonlinear regression analysis to the plot of ΔG_{trans} vs T for the previous data of Woolfson et al. (*38*) and from our own solubility studies gives an estimate of ΔH_{trans} in the range of +22 to +30 kJ mol^{-1} as compared with +3.2 to +12 kJ mol^{-1} for toluene to water. Conversely, considering the analogous transfer of hydrocarbon from aqueous methanol solvent into a hydrophobic close-packed environment suggests a large enthalpic driving force, which is entirely consistent with our measurements on the folding of ubiquitin under these conditions. The linear dependence of protein stability on [MeOH] (Figure 2a) is also mirrored by the linear dependence of ΔG_{trans} for toluene vs [MeOH] (Figure 7), suggesting that methanol perturbs protein stability by increasing the solubility of nonpolar side chains in the unfolded state by reducing the unfavorable solvent-ordering effects associated with the hydrophobic effect.

We have extended the toluene solubility studies to probe the effects of Gdn·HCl on the thermodynamics of folding.

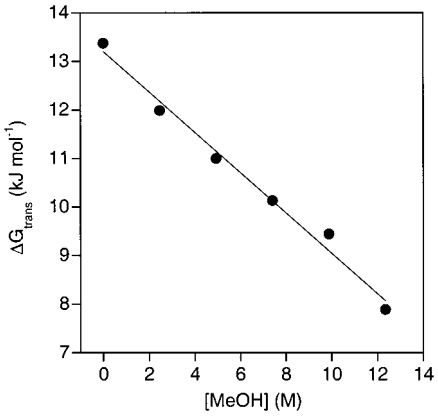

FIGURE 7: Plot of the free energy of transfer from liquid toluene into aqueous methanol solution (ΔG_{trans}) at pH 2.0 as a function of cosolvent concentration at 298 K. The mole fraction of toluene in solution was determined by UV spectrophotometric analysis at 268 nm.

The solubility of toluene is little affected by the presence of 4 M Gdn·HCl in water (unpublished data). Although urea appears to increase the solubility of hydrocarbon (*5*), we find no evidence for this with Gdn·HCl and conclude that the effect of the latter in destabilizing the N and A states of ubiquitin lies largely in its hydrogen bonding capacity rather than on its ability to solvate hydrocarbon. Calorimetry studies on the folding of ubiquitin in the presence and absence of Gdn·HCl suggest that differences in the enthalpy of folding under these different conditions reflect a favorable enthalpic component associated with Gdn·HCl interactions with the unfolded state (*41*).

Furthermore, we examined the solubility of toluene in 40% methanol in the presence of 4 M Gdn·HCl and found that ΔG_{trans} is practically identical to that for transfer into 40% aqueous methanol in the absence of Gdn·HCl. As concluded from the above studies with ubiquitin, the effects of the two denaturants appear to act independently and in an additive sense with Gdn·HCl, not significantly affecting the properties of methanol.

DISCUSSION

Partial Unfolding of Ubiquitin in the Presence of Alcohol Cosolvents. Previously, ubiquitin has been shown to undergo an alcohol-induced transition to a partially folded state (A state) (*48*). This structure is characterized by nativelike α-helical and β-sheet secondary structures in the N-terminal half of the sequence and non-native α-helical structures in the C-terminal portion of the sequence; the latter adopts largely β-sheet structure in the native protein (Figure 1). Detailed NMR structural and dynamic characterization of the A state by a number of groups has shown that these stabilized elements of secondary structure are at best loosely associated, with loss of the majority of nativelike core hydrophobic interactions (*20*, *36*−*38*). Earlier results have shown that the thermodynamics of the N↔A state transition are associated with no significant change in heat capacity at [MeOH] > 30% v/v, suggesting that folding can occur under these conditions in the absence of any significant solvent order effect usually associated with the hydrophobic interaction (*38*). Using Gdn·HCl to destabilize the A state such that the N↔U transition can be observed in the presence of methanol, we have demonstrated that the fully unfolded state can also assemble in a cooperative fashion to a native structure without any significant hydrophobic contribution. The ability of Gdn·HCl to destabilize the A state under these conditions, together with the solvent transfer studies with toluene, strongly suggests that its mode of action as a denaturant hinges primarily on its competitive role in hydrogen bonding to exposed amide groups and stabilizing the unfolded state (*41*, *49*, *50*), rather than on solubilizing hydrocarbon side chains. Studies on the solubility of cyclic dipeptides in urea solutions indicate a favorable enthalpy term associated with urea interactions with polar groups (*5*). These data seem to be in accord with the observation that the unfolding enthalpy change for ubiquitin is lower in the presence of Gdn·HCl than in its absence, indicating enthalpically favorable interactions between the denaturant and the unfolded state (*41*). The magnitude of the difference is, however, subject to some uncertainty due to extrapolation errors from unfolding data at high temperatures.

We have shown that ubiquitin folds cooperatively to the native state under conditions in which the solvent-ordering effects of the hydrophobic interactions are significantly diminished. Despite the fact that conditions can be engineered such that $\Delta G_{N\leftrightarrow U} > 0$, the cooperative integrity of the folded state is preserved in this cocktail of denaturants. By NMR, we see only two clearly resolved states in slow exchange. While burial of core hydrophobic residues and subsequent release of ordered water from nonpolar surfaces is recognized to contribute to protein stability in water, this contribution does not appear to be crucial to the integrity and specificity of the folded state under these conditions despite the suggestion that folding might be highly noncooperative under the dual influence of these two denaturants (*22*).

Thermodynamics of Folding of Model β-Hairpin and α-Helical Peptides. While methanol has a significant destabilizing effect on the tertiary structure of native proteins, the effect on peptides representing isolated elements of secondary structure is to promote folding. In recent work, we have investigated the stability and thermodynamics of β-hairpin formation in a unique system that also shows cold denaturation in water with a maximum stability around 298 K (*51*, *52*). The pronounced curvature of the stability−temperature plot in water is reminiscent of that observed for ubiquitin unfolding in Gdn·HCl, as shown in Figure 3. Again, we observe this plot to become more linear at higher concentrations of methanol, indicative of strongly enthalpy driven β-hairpin folding. $\Delta H_{hairpin}$ and $\Delta S_{hairpin}$ are determined to be close to zero in water alone, with an associated negative ΔC_p for folding. From these data, we concluded that the stability of the folded state in water is largely a consequence of hydrophobic interactions between side chains, for which there is good support from the abundance of side chain nuclear Overhauser effects (NOEs). In 50% methanol, the thermodynamic profile changes completely to become strongly enthalpy driven (*51*). Here, cosolvent promotes folding, as with α-helical peptides, despite the greater solubility of nonpolar side chains in the mixed solvent (loss of hydrophobic effect). By analogy with the data presented here for ubiquitin, we see that ΔC_p for hairpin folding falls essentially to zero under these conditions (*51*) and again conclude that the stabilizing contribution from hydrophobic interactions is significantly diminished. Despite the apparent change in the origin of the interactions stabilizing the β-hairpin

conformation (as reflected in the change in the thermodynamic signature for folding), good side chain packing interactions are again evident from the abundance of interstrand NOEs. The failure of the solvent to significantly perturb the pattern of side chain interactions observed in nuclear Overhauser effect spectroscopy (NOESY) spectra has previously been used as evidence that the effects of cosolvents on stability are manifested through nonspecific effects that destabilize the polypeptide backbone in the unfolded state rather than through explicit solvent−solute interactions (*8*). Thus, in the different solvent milieu, the specificity of the folded state of the β-hairpin, namely, the register of interstrand interactions and location and geometry of the β-turn, remains unaltered. This observation appears to further demonstrate that stereochemical factors (the ϕ and ψ propensity of β-strand and β-turn residues and steric complementarity of side chains) code for the conformational specificity, which is not strongly coupled to the stability of the folded state (*29*).

By analogy, studies of α-helical peptides suggest that cosolvents are most effective in inducing secondary structure in the context of a preexisting helix−coil equilibrium, where the cosolvent cooperatively stabilizes the helix by increasing the α-helical propensity of each residue rather than affecting helix nucleation (*9*, *10*). Using pK_a values for hydroxybenzoic acids to model solvation effects on hydrogen bond strengths shows the latter to mirror cosolvent effects on peptide helical propensities, with both phenomena reaching a plateau above 25% TFE. These data have been suggested to provide strong evidence that an increase in hydrogen bond strength accounts for the increase in helical propensity in TFE (*10*). The folding of β-hairpin peptides reaches a similar plateau in TFE (*53*); however, the effects of methanol appear to operate over a wider concentration range (*51*, *52*). Indeed, the folding of the α-helical peptide from ubiquitin (residues 21−35) appears to be less cooperative in methanol than TFE, requiring a higher concentration of methanol to reach the same folded state, as judged by ellipticity changes at 222 nm (data not shown). Hirato et al. (*27*) reach a similar conclusion in a comprehensive study of effects of alcohols on peptide helicity. The data suggest that, in the presence of cosolvents, hydrogen bonds in model α-helices and β-hairpins approach nativelike strengths, the energetic benefit of which more than offsets any loss of the contribution from the hydrophobic effect and van der Waals interactions that are simultaneously incurred by the change in solvent composition. In contrast, as described above, cosolvent appears to destabilize native states of proteins because hydrogen bond strengths in the folded state (which are already close to optimum) are not sufficiently enhanced to offset the large loss of free energy contributed by the hydrophobic effect and van der Waals interactions from burial of nonpolar residues. It has been noted that, while the effect of TFE on helix stability reaches a plateau above 25%, the T_m of proteins shows a linear depression as a function of alcohol content (*54*). We have similarly noted here that both $\Delta G_{N\leftrightarrow U}$ and $\Delta H_{N\leftrightarrow U}$ vs [MeOH] for ubiquitin folding also show linear correlations with the enthalpy term becoming increasingly negative. This correlates well with the linear dependence of the solubility of toluene (ΔG_{trans}) on cosolvent concentration described above, suggesting that the solvent effects on the solubility of nonpolar side chains dominates the effects on protein stability.

Energetics of the N↔U vs N↔A Transitions of Ubiquitin. On the basis of the thermodynamic data for the N↔U vs N↔A transitions, we have attempted to draw some conclusions regarding the contribution of the various interaction terms in the presence and absence of methanol. On the basis of the model of the A state described by Brutscher et al. (*37*) (see Figure 1), we conclude that the number of hydrogen bonding interactions in the N state and the A state is very similar ($\Delta N_{HB}{}^{N\leftrightarrow A} \approx 0$). The secondary structure composition in the N-terminal portion of the sequence is nativelike in the A state, but the C-terminal portion of the sequence has solvent-induced non-native helical structure, as compared with mainly β-sheet composition in the native structure. To a first approximation, the major structural differences between the N state and the A state relate to the absence in the latter of a packed nonpolar core. It is interesting that the N↔A and N↔U transitions, both of which involve formation of the protein core, are associated with a similar large enthalpy change in high concentrations of methanol. As far as the contribution of hydrogen bonding is concerned, the fact that $\Delta N_{HB}{}^{N\leftrightarrow A} \approx 0$ but $\Delta N_{HB}{}^{N\leftrightarrow U} \gg 0$ seems to have only a minor effect on the enthalpy of formation of the native state under these conditions, suggesting that hydrogen bonding interactions have a relatively small net enthalpic contribution to the N↔U transition in the presence of the cosolvent and Gdn·HCl. We conclude that the origin of the large enthalpic driving force for both the N↔A and the N↔U transitions in high concentrations of cosolvents arise from the same source, van der Waals packing of nonpolar residues in the protein core. The sign and magnitude of transfer enthalpies for toluene into aqueous methanol solutions are in agreement with this conclusion (see above and ref *38*). Thus, use of cosolvents to examine the thermodynamics of folding has enabled us to strip away the entropic contribution from the hydrophobic effect and examine the folding transition under conditions in which van der Waals packing appears to dominate the free energy of the folding process. Thus, formation of core nonpolar interactions provides a sufficient driving force for folding, and the entropic benefit associated with solvent release (hydrophobic interactions) does not appear to be a prerequisite for folding.

In support of these conclusions, recent studies of the thermodynamics of protein folding in the RNase S protein−peptide complex have considered mutations that locally disrupt packing interactions in the folded state and have concluded that van der Waals interactions, rather than hydration (hydrophobic) effects, are largely responsible for the change in stability of the mutants in water. For example, mutation of Phe8 to smaller residues results in a large enthalpic destabilization and entropic changes opposite to those expected from the hydrophobic effect (*55*). A variety of thermodynamic data on the solubility of model compounds has also concluded that the dominant contribution of nonpolar side chains to protein stability is van der Waals packing interactions rather than hydration effects (*5*, *56*).

In conclusion, we have shown that although the conformational equilibrium between folded and unfolded states of ubiquitin is readily perturbed by the solvent environment, resulting in a change in the thermodynamic signature for folding, the source of conformational specificity is clearly

robust and widely distributed within the primary sequence (*29*), allowing the protein to fold in a highly cooperative manner, even when a major source of stability driving the folding transition has been largely negated.

ACKNOWLEDGMENT

We thank Sam Griffiths-Jones for some preliminary measurements on the N↔A transition.

REFERENCES

1. Myers, J. K., Pace, C. N., and Scholtz, J. M. (1995) *Protein Sci. 4*, 2138−2148.
2. Pace, N. C., and Scholtz, J. M. (1997) *Protein Structure−A Practical Approach* (Creighton, T. E., Ed.) 2nd ed., IRL Press, New York.
3. Wallqvist, A., Covell, D., and Thirumalai, D. (1998) *J. Am. Chem. Soc. 120*, 427−428.
4. Vanzi, F., Madan, B., and Sharp, K. (1998) *J. Am. Chem. Soc. 120*, 10748−10753.
5. Zou, Q., Habermann-Rottinghaus, S., and Murphy, K. (1998) *Proteins*: *Struct., Funct., Genet. 31*, 107−115.
6. Nelson, J. W., and Kallenbach, N. R. (1986) *Proteins*: *Struct., Funct., Genet. 1*, 211−217.
7. Sonnichsen, F. D., Van Eyk, J. E., Hodges, R. S., and Sykes, B. D. (1992) *Biochemistry 31*, 8790−8798.
8. Storrs, R. W., Truckses, D., and Wemmer, D. E. (1992) *Biopolymers 32*, 1695−1702.
9. Jasanoff, A., and Fersht, A. R. (1994) *Biochemistry 33*, 2129−2135.
10. Luo, P., and Baldwin, R. L. (1997) *Biochemistry 36*, 8413−8421.
11. Bolin, K. A., Pitkeathly, M., Miranker, A., Smith, L. J., and Dobson, C. M. (1996) *J. Mol. Biol. 261*, 443−453.
12. Blanco, F. J., Jimenez, M. A., Pineda, A., Rico, M., Santoro, J., and Nieto, J. L. (1994) *Biochemistry 33*, 6004−6014.
13. Cox, J. P. L., Evans, P. A., Packman, L. C., Williams, D. H., and Woolfson, D. N. (1993) *J. Mol. Biol. 234*, 483−492.
14. Searle, M. S., Zerella, R., Williams, D. H., and Packman, L. C. (1996) *Protein Eng. 9*, 559−565.
15. Kentsis, A., and Sosnick, T. R. (1998) *Biochemistry 37*, 14613−14622.
16. Hirato, N., Mizuno, K., and Goto, Y. (1997) *Protein Sci. 6*, 416−421.
17. Buck, M., Radford, S. E., and Dobson, C. M. (1993) *Biochemistry 32*, 669−678.
18. Alexandrescu, A. T., Ng, Y.-L., and Dobson, C. M. (1994) *J. Mol. Biol. 235*, 587−599.
19. Shiraki, K., Nishikawa, K., and Goto, Y. (1995) *J. Mol. Biol. 245*, 180−194.
20. Harding, M., Williams, D. H., Evans, P. A., and Woolfson, D. N. (1991) *Biochemistry 30*, 3120−3128.
21. Hamada, D., and Goto, Y. (1997) *J. Mol. Biol. 269*, 479−487.
22. Buck, M. (1998) *Q. Rev. Biophys. 31*, 297−355.
23. Main, E. R. G., and Jackson, S. E. (1999) *Nat. Struct. Biol. 6*, 831−835.
24. Hamada, D., Chiti, F., Guijarro, J. I., Kataoka, M., Taddei, N., and Dobson, C. M. (2000) *Nat. Struct. Biol. 7*, 58−61.
25. Yiu, C. P. B., Mateu, M. G., and Fersht, A. R. (2000) *ChemBioChem 1*, 49−55.
26. Walgers, R., Lee, T. C., and Cammers-Goodwin, A. (1998) *J. Am. Chem. Soc. 120*, 5073−5079.
27. Hirato, N., Mizuno, K., and Goto, Y. (1998) *J. Mol. Biol. 275*, 365−378.
28. Anderson, N. H., Cort, J. R., Liu, Z., Sjoberg, S. J., and Tong, H. (1996) *J. Am. Chem. Soc. 118*, 10309−10310.
29. Lattman, E. E., and Rose, G. D. (1993) *Proc. Natl. Acad. Sci. U.S.A. 90*, 439−441.
30. Dill, K. A. (1990) *Biochemistry 29*, 7133−7141.
31. Honig, B. (1999) *J. Mol. Biol. 293*, 283−293.
32. Robertson, A. D., and Murphy, K. P. (1997) *Chem. Rev. 97*, 1251−1267.
33. Vijay-Kumar, S., Bugg, C. E., and Cook, W. J. (1987) *J. Mol Biol. 194*, 531−544.
34. Di Stefano, D. L., and Wand, A. J. (1987) *Biochemistry 26*, 7272−7281.
35. Weber, P. L., Brown, S. C., and Mueller, L. (1987) *Biochemistry 26*, 7282−7291.
36. Stockman, B., Euvrard, A., and Scahill, T. A. (1993) *J. Biomol. NMR 3*, 285−296.
37. Brutscher, B., Bruschweiler, R., and Ernst, R. R. (1997) *Biochemistry 36*, 13043−13053.
38. Woolfson, D. N., Cooper, A., Harding, M. M., Williams, D. H., and Evans, P. A. (1993) *J. Mol. Biol. 229*, 502−511.
39. Briggs, M. A., and Roder, H. (1992) *Proc. Natl. Acad. Sci. U.S.A. 89*, 2017−2021.
40. Jourdan, M., and Searle, M. S. (2000) *Biochemistry 39*, 12355−12364.
41. Ibarra-Molero, B., Makatadze, G. I., and Sanchez-Ruiz, J. M. (1999) *Biochim. Biophys. Acta 1429*, 384−390.
42. Ibarra-Molero, B., Makatadze, G. I., and Sanchez-Ruiz, J. M. (1999) *Biochemistry 38*, 8138−8149.
43. Wintrode, P. L., Makhatadze, G. I., and Privalov, P. L. (1994) *Proteins*: *Struct., Funct., Genet. 18*, 246−253.
44. Horn, J. R., Russell, D., Lewis, E. A., and Murphy, K. P. (2001) *Biochemistry 40*, 1774−1778.
45. Murphy, K. P., and Gill, S. J. (1991) *J. Mol. Biol. 222*, 3, 699−709.
46. Murphy, K. P., Privalov, P. L., and Gill, S. J. (1990) *Science 247*, 4942, 559−561.
47. Baldwin, R. L. (1986) *Proc. Natl. Acad. Sci. U.S.A. 83*, 8069−8072.
48. Wilkinson, K. D., and Mayer, A. N. (1986) *Arch. Biochem. Biophys. 250*, 390−394.
49. Makhatadze, G. I., and Privalov, P. L. (1992) *J. Mol. Biol. 226*, 491−505.
50. Pace, N. C., and Tanford, C. (1968) *Biochemistry 7*, 198−208.
51. Maynard, A. J., Sharman, G. J., and Searle, M. S. (1998) *J. Am. Chem. Soc. 120*, 1996−2007.
52. Griffiths-Jones, S. R., Maynard, A. J., and Searle, M. S. (1999) *J. Mol. Biol. 292*, 1051−1069.
53. Ramirez-Alvarado, M., Blanco, F. J., and Serrano, L. (1996) *Nat. Struct. Biol. 3*, 604−612.
54. Cinelli, S., Onori, G., and Santucci, A. (1997) *J. Phys. Chem. B 101*, 8029−8034.
55. Ratnaparkhi, G. S., and Varadarajan, R. (2000) *Biochemistry 39*, 12365−12374.
56. Makhatadze, G. I., and Privalov, P. L. (1995) *Adv. Protein Chem. 47*, 307−425.
57. Koradi, R., Billeter, M., and Wuthrich, K. (1996) *J. Mol. Graphics 14*, 51−55.

BI010767J